Mathematical Biosciences and Engineering

http://www.aimspress.com/journal/MBE

MBE, 17(4): 4034–4047.
DOI: 10.3934/mbe.2020223
Received: 03 March 2020
Accepted: 27 May 2020
Published: 03 June 2020

Research article

The impact of media on the spatiotemporal pattern dynamics of a reaction-diffusion epidemic model

Xin-You Meng*and Tao Zhang

School of Science, Lanzhou University of Technology, Lanzhou, Gansu 730050, China

* **Correspondence:** Email: xymeng@lut.edu.cn.

Abstract: In this paper, a reaction-diffusion SI epidemic model with media impact is considered. The boundedness of system and the existence of the state are given. The local stabilities of the endemic states are analyzed. Sufficient conditions of the occurrence of the Turing pattern are obtained by the center manifold theorem and normal form method. Some numerical simulations are given to check in the theoretical results. We find that the influence of media not only inhibits the spread of infectious diseases, but also effects the spatial steady-state of model.

Keywords: epidemic model; media impact; spatiotemporal distribution; Turing instability

1. Introduction

In epidemiology, mathematical model is an important method for quantitative analysis of the spread and control of infectious diseases [1, 2, 3]. Lots of epidemiological models have been established to understand the mechanism of disease transmission based on some diseases, such as cholera [4], Ebola [5], alzheimer's disease [6], sexually transmitted diseases [7]. Some models are given by considering different factors, such as the incidence rate [8, 9, 10, 11], infectious diseases transmission [12, 13], cross-diffusion [14, 15, 16], seasonal variation [17], vaccination [18, 19, 20], control [21, 22], multiplex network [23], different patches [24, 25] and other factors [26, 27, 28]. Those results are useful to predict the development trend of infectious diseases, identify the key factors of transmission, and seek the best strategies to control the spread of infectious diseases.

By dividing the total population N into the susceptible population S and the infectious population I, Berezovskaya et al. [29] introduced a simple epidemic model as follows

$$\begin{cases} \dfrac{\mathrm{d}S(t)}{\mathrm{d}t} = rN(1-\dfrac{N}{K}) - \dfrac{\beta S(t)I(t)}{N} - (\mu+m)S(t), \\ \dfrac{\mathrm{d}I(t)}{\mathrm{d}t} = \dfrac{\beta S(t)I(t)}{N} - (\mu+d)I(t), \end{cases} \tag{1.1}$$

where the birth process incorporates the effects of density dependent by a logistic equation with the intrinsic growth rate r and the carrying capacity K. β denotes the transmission rate (the infection rate is constant), μ is the natural mortality rate; d denotes the disease-induced mortality rate and m is the per-capita emigration rate of uninfected. What's more, some diseases are taken into account the population models from the view point of mathematical epidemiology in recent years [30, 31, 32, 33].

The spatial epidemic models showing the rich dynamics of disease transmission, have been received more and more attention. Such as, Wang et al. [34] investigated the complex dynamics of a reaction diffusion SI model incorporating demographic and epidemiological processes with zero-flux boundary conditions. Their results indicate that the diffusion has a great influence on the spread of the epidemic and extend well the finding of spatiotemporal dynamics in the epidemic model. Wang [35] investigated the pattern dynamics of a spatial epidemic model with logistic growth. By using amplitude equation, they found that there were different types of stationary patterns including spotted, mixed, and stripe patterns, which mean that the individual movement in the space can lead to a high density of disease. Many other scholars done similar work . By taking diffusion into model (1.1), Wang et al.[36] proposed the model with the form of the partial differential equation as follows

$$\begin{cases} \dfrac{\partial S(t)}{\partial t} = rN(1-\dfrac{N}{K}) - \dfrac{\beta S(t)I(t)}{N} - (\mu+m)S(t) + d_1\nabla^2 S, \\ \dfrac{\partial I(t)}{\partial t} = \dfrac{\beta S(t)I(t)}{N} - (\mu+d)I(t) + d_2\nabla^2 I. \end{cases} \tag{1.2}$$

They presented Turing pattern selection in a model (1.2) under zero-flux boundary conditions. In addition, some authors also investigated the pattern dynamics of models, such as [37, 38, 39].

Media impact has a particularly significant effect on reducing the infection rate of infectious diseases [40, 41, 42]. With the spread of the epidemic, this reduction of the infection rate becomes weaker and weaker, and the susceptible population can not form new habits to avoid infection. That is, the number of infected people has a critical value. At this critical point, the number of the susceptible population changing their behaviors reach the maximum, which shows that the reduction of media impact reaches the maximum. With the continuous increase of the number of patients, the susceptible population still need to participate in some necessary social activities to contact other people. Modelling the media impact on the spread of disease shares tremendous popularity in these years. Thus, some scholars introduced epidemic model with media impact [43, 44, 45]. Liu et al.[43] described the media coverage impact on the transmission dynamic including a describing factor $\beta e^{-a_1E-a_2I-a_3H}$ in the transmission coefficient, here E, I, *and* H are the numbers of reported exposed, infectious, and hospitalized individuals, respectively. Cui et al. [44] used $c_1 - c_2 f(I)$ as the contact rate to investigate the effect of media coverage on the spread of disease and obtained that the media coverage was important on the spread of the infectious disease. Further, Liu and Cui [45] considered a model with media coverage as follows

$$\begin{cases} \dfrac{\mathrm{d}S(t)}{\mathrm{d}t} = r - dS - (\beta_1 - \beta_2\dfrac{I}{m+I})SI + \delta R, \\ \dfrac{\mathrm{d}I(t)}{\mathrm{d}t} = (\beta_1 - \beta_2\dfrac{I}{m+I})SI - (d+\gamma+\alpha)I, \\ \dfrac{\mathrm{d}R(t)}{\mathrm{d}t} = \gamma I - (d+\delta)R. \end{cases} \tag{1.3}$$

Where $\beta(I) = \beta_1 - \beta_2\frac{I}{m+I}$ is the contact rate after media alert. β_1 denotes the contact rate before media

alert, and $\beta_2\frac{I}{m+I}$ reflects the reduced value of the transmission rate when infectious individuals appear and are reported. β_2 is the maximum value of the transmission rate, m reflects the reactive velocity of people and media coverage to the disease. Li and Cui [46] also considered an SIS epidemic model with pulse vaccination and incidence rate $\beta(I) = \beta_1 - \beta_2\frac{I}{m+I}$.

In addition, Cui et al. [47] formulated a compartment model with incidence rate μe^{-mI} with m reflecting the impact of media coverage on transmission dynamics, and obtained that Hopf bifurcation exists when m is sufficiently small. Recently, Xiao et al. [48] formulated the media function depending on switch on and off in a highly nonlinear fashion with the greatest effect during the early stage of the outbreak. Yan et al. [49] presented a novel methodology by using cross-correlation analysis and embedding a media function and the number of news reports into classical SEIR model, showed that combining statistical analysis with a mathematical model was beneficial to analyze media impacts. Moreover, other forms, such as $\mu_1 - \mu_2 f(I)\frac{SI}{S+I}$, have been proposed to describe the media-induced incidence rate (see details in [50, 51]).

Based on the above work [45, 47], we think that the effect of media reports is different in different period of infectious diseases. The impact of media reports on the disease is relatively large when the number of infected people is small, but the impact of media reports on the disease is relatively weak when the number of infected people is large. Thus, we take media impact into account the model (1.2), which can be described by

$$f(I(t)) = \frac{1}{1+\beta\alpha I(t)},$$

here α is the influencing factor ($\alpha > 0$) reflecting the impact of media coverage the effective contact rate. This function can also be interpreted as the influencing factor function decreasing exponentially with the increase of the number of infected persons when the number of infected persons is less than the critical value. However, once the number of the infected reaches or exceeds this critical value, this function will be interpreted as the influencing factor [45].

Based on the above factors, the following model is given

$$\begin{cases} \dfrac{\partial S(t)}{\partial t} = rN(1-\dfrac{N}{K}) - \dfrac{1}{1+\beta\alpha I(t)}\dfrac{\beta S(t)I(t)}{N} - (\mu+m)S(t) + d_1\nabla^2 S(t), \\ \dfrac{\partial I(t)}{\partial t} = \dfrac{1}{1+\beta\alpha I(t)}\dfrac{\beta S(t)I(t)}{N} - (\mu+d)I(t) + d_2\nabla^2 I(t). \end{cases} \tag{1.4}$$

Model (1.4) will be analysed under the following non-zero initial condition

$$S(r,0) > 0, \quad I(r,0) > 0, \quad r = (x,y) \in \Omega = [0,L]\times[0,L],$$

and zero-flux boundary condition

$$\frac{\partial S}{\partial n} = \frac{\partial I}{\partial n} = 0.$$

As far as we know, media impact taken into models with partial differential equations (PDEs) is less than the other cases. Especially, there are few studies including both spatial diffusion and media influence in the spatial infectious disease model. For this purpose, we will make a detailed analysis of a spatial disease model with media impact.

The main contents of this paper are as follows. In part two, we will show the stability of each equilibrium point. In the third section, we will obtain the conditions under which Turing instability

occurs. In addition, we will carry out numerical simulations to verify our theoretical results. Some conclusions and discussions are given in the end.

2. Boundaries and the existence of equilibrium state

The basic demographic reproductive number R_d is given by $R_d = \frac{r}{\mu+m}$. It can be shown that if $R_d > 1$, then the population grows, inverse the population does not survive.

The basic reproductive number is $R_0 = \frac{\beta}{\mu+d}$ according to the method of reference [52]. Generally speaking, the disease will invade successfully when $R_0 > 1$, but it will die out if $R_0 < 1$.

Re-scaling the model (1.4) by letting $S \to \frac{S}{K}$, $I \to \frac{I}{K}$, $t \to \frac{t_1}{\mu+d}$, for convenience, we still write t_1 down as t, which leads to the following model without diffusion

$$\begin{cases} \dfrac{\mathrm{d}S(t)}{\mathrm{d}t} = \vartheta R_d(S+I)(1-(S+I)^2) - \dfrac{R_0}{1+\beta\alpha KI}\dfrac{SI}{S+I} - \vartheta S, \\ \dfrac{\mathrm{d}I(t)}{\mathrm{d}t} = \dfrac{R_0}{1+\beta\alpha KI}\dfrac{SI}{S+I} - I. \end{cases} \tag{2.1}$$

Where $\vartheta = \frac{\mu+m}{\mu+d}$ is the ratio of the average life-span of susceptible to that of infectious.

Re-scaling the model (2.1) by letting $\mathrm{d}t \to (S+I)\mathrm{d}t$ leads to the following model

$$\begin{cases} \dfrac{\mathrm{d}S(t)}{\mathrm{d}t} = \vartheta R_d(S+I)^2(1-(S+I)^2) - \dfrac{R_0SI}{1+\beta\alpha IK} - \vartheta(S+I)S, \\ \dfrac{\mathrm{d}I(t)}{\mathrm{d}t} = \dfrac{R_0SI}{1+\beta\alpha IK} - (S+I)I. \end{cases} \tag{2.2}$$

We assume that the susceptible S and infectious population I move randomly, described as Brown random motion. Thus, corresponding to model (2.2), we propose a simple spatial model as follows

$$\begin{cases} \dfrac{\partial S(t)}{\partial t} = \vartheta R_d(S+I)^2(1-(S+I)^2) - \dfrac{R_0SI}{1+\beta\alpha IK} - \vartheta(S+I)S + d_1\nabla^2 S, \\ \dfrac{\partial I(t)}{\partial t} = \dfrac{R_0SI}{1+\beta\alpha IK} - (S+I)I + d_2\nabla^2 I, \end{cases} \tag{2.3}$$

where the nonnegative constants d_1 and d_2 are the diffusion coefficients of S and I, respectively. The usual Laplace operator in two dimensional space $\nabla^2 = \frac{\partial^2}{\partial x^2} + \frac{\partial^2}{\partial y^2}$, is used to describe the Brown random motion.

Model (2.3) is to be analysed under the following non-zero initial conditions

$$S(r,0) > 0, \quad I(r,0) > 0, \quad r = (x,y) \in \Omega = [0,L] \times [0,L], \tag{2.4}$$

and zero-flux boundary conditions

$$\frac{\partial S}{\partial n} = \frac{\partial I}{\partial n} = 0,$$

where L denotes the size of the system in the directions of x and y, n is the outward unit normal vector of the boundary $\partial\Omega$. The main reason for choosing such boundary conditions is that we are interested in the self-organization of patterns. Zero-flux boundary conditions imply that there is no flux of population through the boundary, that is, no external input is imposed from outside.

Next, we will investigate some preliminary and relevant properties of the system (2.3). The methods for the existence of the solutions can be found in the references [38, 53, 54].

It is obvious that system (2.3) has one zero equilibrium $E_0 = (S_0, I_0) = (0, 0)$. If $R_d > 1$, then system (2.3) has one boundary equilibrium $E_1 = (S_1, I_1) = (\sqrt{\frac{R_d-1}{R_d}}, 0)$.

From the second equation of system (2.3), we have that

$$S = \frac{I(1+\beta\alpha KI)}{R_0 - (1+\beta\alpha KI)}. \tag{2.5}$$

By submitting (2.5) into the first equation of system (2.3), we have that

$$\begin{aligned} &\vartheta(R_d - I)(R_d - \xi)^4 + (R_d - \xi)^3(\vartheta R_d\xi I - 4\xi I^3 - R_0 - \vartheta\xi I) - \\ &\vartheta R_d(R_0 - \xi)^2 I(1 - I^2) - 4(R_0 - \xi)^3 - 4R_d\xi^4 I^3 = 0, \end{aligned} \tag{2.6}$$

where $\xi = 1 + \beta\alpha KI$.

Due to the complexity of Eq.(2.5), it is difficult to obtain the exact solutions to Eq.(2.5). Thus, we give one assumption as follows

(H_0): Eq.(2.5) has one positive root.

Thus, system (2.3) has one positive equilibrium $E_* = (S_*, I_*)$, where S_* and I_* satisfy the following

$$\begin{aligned} &S_* = \frac{\xi I_*}{R_0 - \xi}, \\ &\vartheta(R_d - I_*)(R_d - \xi)^4 + (R_d - \xi)^3(\vartheta R_d\xi I_* - 4\xi I_*^3 - R_0 - \vartheta\xi I_*) - \\ &\vartheta R_d(R_0 - \xi)^2 I_*(1 - I_*^2) - 4(R_0 - \xi)^3 - 4R_d\xi^4 I_*^3 = 0, \end{aligned}$$

where $\xi = 1 + \beta\alpha KI_*$.

In the following, we will investigate the local stability of system (2.2).

Theorem 2.1. *All the non-negative solutions of model (2.2) that start in R_+^2 are bounded, with ultimate bound independent of the initial conditions.*

Proof. Denoting $W(t) = S(t) + I(t)$, we have

$$\frac{\mathrm{d}W(t)}{\mathrm{d}t} = \vartheta R_d(S + I)^2(1 - (S + I)^2) - (S + I)(\vartheta S + I).$$

For each $\eta > 0$, the following inequality

$$\begin{aligned} \frac{\mathrm{d}W(t)}{\mathrm{d}t} + \eta W &= \vartheta R_d((S + I)^2 - (S + I)^4) - (S + I)(\vartheta S + I - \eta) \\ &\leq \vartheta R_d(W^2 - W^4) - W(\vartheta S + I - \eta) \end{aligned}$$

is true. By taking $\eta < \min\{R_d, \vartheta, 1\}$, the right-hand side of the above inequality is bounded. That is

$$\frac{\mathrm{d}W(t)}{\mathrm{d}t} \leq (\vartheta R_d W - \eta - \vartheta R_d W^3)W.$$

There exists a T, such that for $t > T$,

$$\limsup_{t\to\infty} W(t) \leq 1 - \frac{\eta}{\vartheta R_d}.$$

It is easy to see that is independent of the initial condition. We conclude the proof. □

3. Stability analysis and Turing bifurcation

3.1. Stability analysis of the disease-free state

The linearized system of system (2.3) at the coexistence state E_* is as follows

$$\begin{cases} \dfrac{\partial S(t)}{dt} = a_{311}S + a_{312}I + d_1\nabla^2 S, \\ \dfrac{\partial I(t)}{dt} = a_{321}S + a_{322}I + d_2\nabla^2 I, \end{cases} \tag{3.1}$$

where

$$\begin{aligned} a_{311} &= \vartheta R_d[2S_*(S_* + I_*) - 4S_*(S_* + I_*)^3] - \frac{R_0 I_*}{1 + \beta\alpha K I_*} - \vartheta(2S_* + I_*), \\ a_{312} &= \vartheta R_d[2I_*(S_* + I_*) - 4I_*(S_* + I_*)^3] - \frac{R_0 S_*}{(1 + \beta\alpha K I_*)^2} - \vartheta S_*, \\ a_{321} &= \frac{R_0 S_* I_*}{1 + \beta\alpha K I_*} - I_*(S_* + I_*), \\ a_{322} &= \frac{R_0 S_*}{(1 + \beta\alpha K I_*)^2} - \vartheta S_*. \end{aligned}$$

Let

$$\begin{pmatrix} S \\ I \end{pmatrix} = \begin{pmatrix} \alpha_1 \\ \alpha_2 \end{pmatrix} \exp(\lambda t + i\overrightarrow{\mathrm{k}_c}\,\overrightarrow{r}), \tag{3.2}$$

where $\overrightarrow{\mathrm{k}_c} = (k_x, k_y)$, $\overrightarrow{r} = (x, y)$, λ is the growth rate of perturbation at time t, and $\mathrm{k}_c = \sqrt{k_x^2 + k_y^2}$ is the number of the wave.

Substituting (3.2) into (3.1), we can obtain that the characteristic equation is

$$\lambda^2 + g_1(\mathrm{k}_c)\lambda + g_2(\mathrm{k}_c) = 0, \tag{3.3}$$

where

$$\begin{aligned} g_1(\mathrm{k}_c) &= d_1 k_c^2 + d_2 k_c^2 - a_{311} - a_{322}, \\ g_2(\mathrm{k}_c) &= d_1 d_2 k_c^4 - a_{311} d_2 k_c^2 - a_{322} d_1 k_c^2 + a_{311}a_{322} - a_{312}a_{321}. \end{aligned}$$

In the case of system (2.3) without diffusion, the corresponding characteristic equation is as follow

$$\lambda^2 + g_1(0)\lambda + g_2(0) = 0, \tag{3.4}$$

where

$$g_1(0) = -a_{311} - a_{322}, \quad g_2(0) = a_{311}a_{322} - a_{312}a_{321}.$$

According to the *Routh − Hurwitz*, the necessary and sufficient condition for the stability of the local equilibrium state E_* is that the real part of all eigenvalues is less than zero. It follows that

$$(H_1) : g_1(0) > 0,$$

$$(H_2) : g_2(0) > 0.$$

Thus, the coexistence state E_* is stable when $R_0 > 1$, (H_1) and (H_2) are true.

The necessary condition for the occurrence of the Turing pattern is that system (2.3) is stable in the absence of diffusion, but the coexistence state E_* of system (2.3) with diffusion is unstable. The condition for occurrence of the Turing branch from the coexistence state E_* will be given detailed in the next.

3.2. Analysis of Turing bifurcation

In 1953, Turing(1952) showed that a system including coupled reaction-diffusion equations can be used to describe patterns in biological system. $Turing^{'}s$ theory shows that the interplay of chemical reaction and diffusion may cause the local stability of system to be unstable for the diffusive system and lead to the spontaneous formulation of a spatially periodic stationary structure. This kind of instability is called Turing instability or diffusive-driven instability.

In this part, we will derive some conditions for the Turing instability for the spatially homogeneous equilibrium solution to system (2.3).

Case 1 $g_1(k_c) > 0$.

Since all diffusion coefficients are positive, the Turing pattern takes place under such **Case 1**.

Case 2. $g_2(k_c) > 0$.

Let $z = k_c^2$. We have that

$$g_2(z) = h_1 z^2 - h_2 z + h_3,$$

where $h_1 = d_1 d_2$, $h_2 = a_{311} d_2 + a_{322} d_1$, $h_3 = a_{311} a_{322} - a_{321} a_{312}$.

We can obtain that the minimum point of $g_2(z)$ is $z_{min} = \frac{h_2}{2h_1}$. Since z_{min} represents a physical wave number, $z_{min} = \frac{h_2}{2h_1}$ is positive. Thus, the sufficient conditions of the Turing branch taking place are the assumptions (H_1), (H_2) and

$(H_3) : z_{min} = \frac{h_2}{2h_1} > 0, \;\; g_2(z_{min}) = g_2(\frac{h_2}{2h_1}) = \frac{h_1 h_3 - h_2^2}{4h_1} < 0$

hold.

4. Numerical simulation

In this section, we select parameters satisfied the assumptions (H_1) and (H_2), simulate the steady-state pattern of system (2.3). The values of all parameters are $d_1 = 0.01, d_2 = 0.25, \vartheta = 0.15, \mu = 0.000001, d = 0.0000005, m = 0.000001, r = 0.0000024, \beta = 0.000003, K = 20000$. The influence of the change of transmission mode on transmission parameters is also studied. The information contained in infectious diseases and the hidden information behind Turing mode are revealed. For this purpose, the space area is $[0, 100] \times [0, 100]$, and the time interval is $[0, 50000]$. The space step is $\Delta h = 1$, and the time step is $\Delta t = 0.01$. The initial value is the random perturbation value of the coexistence state E_*, and the boundary is Neumann boundary condition. In system (2.3), we pay more attention to the evolution and distribution of space diseases.

When we keep the other parameters unchanged and take the media coefficients with different values, we can observe how the media affect the system. The reaction is mainly expressed by different patches, but media influences are given different values which are not randomly chosen. But after repeated debugging, we can get the following four patterns, which can be seen in Fig 1, Fig 2, Fig 3 and Fig 4.

The evolution process is wide stripes to mixed stripes and spots, to only spots, and they are the steady-state patterns. The numerical simulation results show that the density of the infected population tends to a certain value with time increasing. The density of infected people may vary in different locations.

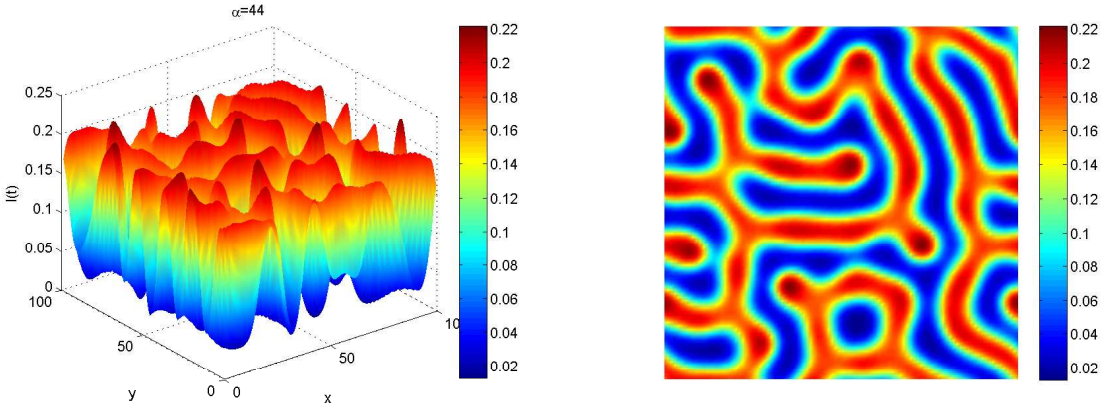

(a) (b)

Figure 1. When media coefficient is $\alpha = 44$, the system has a thick stripe pattern.

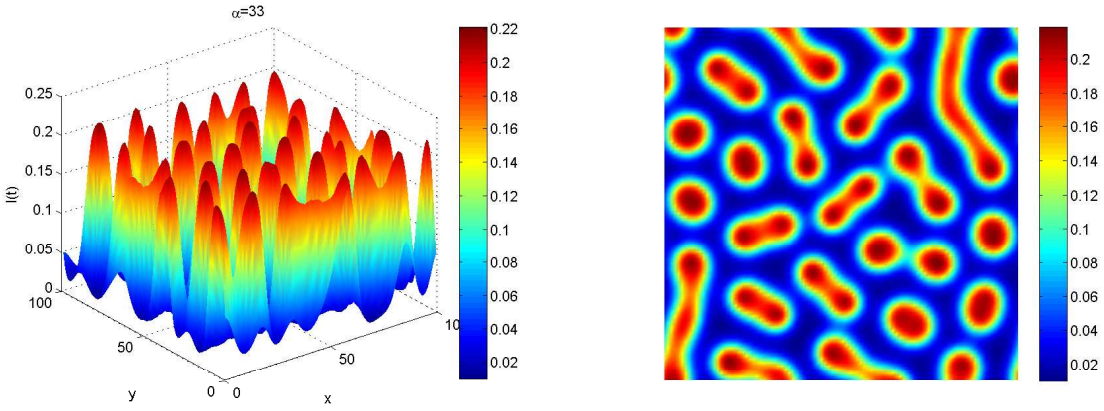

(a) (b)

Figure 2. When media coefficient is $\alpha = 33$, the system has a mixed pattern of spots and stripes.

From the under numerical simulations, we can clearly observe that the change of media impact causes the structures to change the Turing pattern. When the parameter $\alpha \geq 80$, there is no change in the Turing mode, which means that the influence of media is too small, and the system dose not change. When the parameter α is smaller than 80, that is, the influence of media becomes larger, the Turing mode changes gradually from wide stripes to stripes and spots mixed state, and finally to the state of only spots. Finally, when the media coefficients exceed a certain value, the system does not change. That is, the influence of media impact on disease has a certain range.

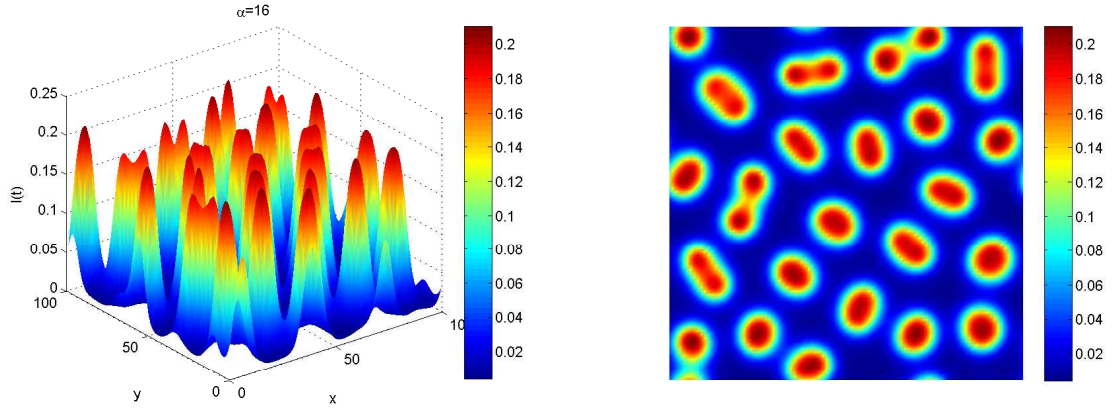

(a) (b)

Figure 3. When media coefficient is $\alpha = 16$, the system has a spot pattern.

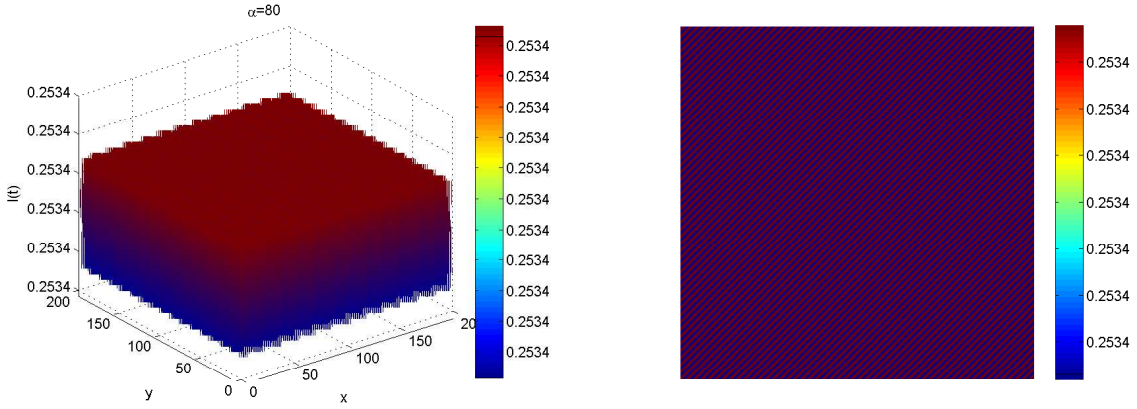

(a) (b)

Figure 4. When media coefficient is $\alpha = 80$, the system no longer changes with the change of media coefficient

5. Conclusions

Media communications have a great impact on individual behaviour changes, therefore significantly impact on the spread and outbreak of infectious disease. In recent years, models associated with the impact of media coverage on disease spread show a tremendous popularity. However, these models ignore the lag effect of media impact on the spread of infectious disease. Thus, a model of the lag effect of media impact is analyzed and discussed in this paper.

In model (1.2), Wang et al.[36] studied Turing pattern, and spent a lot of time to study solutions and its properties. The SI infectious disease model with media impact is studied in this paper. Necessary conditions of Turing pattern are obtained by Eq.(3.3). Focusing on the bifurcation conditions of Eq.(3.3), we studied the effects of media on infections diseases by numerical simulations with media impact as parameters. The results showed that the average spatial density of infected population

decreases with the increase of media influence.

By comparison, we mainly study this system consisting of media impact. It is worthy that the shape of the pattern represents the actual distribution of infectious diseases. Through understanding the structure of the model, we can clearly observe that the change of media impact causes the structures to change the Turing pattern. When the parameter α varies, the influence of media becomes larger, the Turing mode changes gradually from wide stripes to stripes and spots mixed state, and finally to the state of only spots. But when the parameter α is less or bigger than one value, such system does not change. That is to say, the influence of media impact on disease has a certain range. Thus, we can take some measures for the prevention and control of infectious diseases. The results also enrich the dynamics of media impact reaction-diffusion epidemic models.

The new coronary pneumonia that broke out in 2020. After understanding the pathogenic mechanism of the new coronavirus. After the transmission route and infection mode, the country immediately took extremely strong prevention and control measures. Take closed management of the city of Wuhan. This is the first time such a measure has been taken in a city with a population of 20 million since the founding of the People's Republic of China. It first controlled the output fluidity of the disease source, that is, to control the flow of infected people into susceptible people. Especially active and effective, the next step is to let people wear masks and wash their hands frequently. Since the main infection of this new coronavirus is infection through contact infection from the respiratory tract, this time wearing a mask is the most effective for individuals to prevent infection effective way. After having these extremely strong protective measures, the next step is to let susceptible individuals know the effective measures. In the 21st century, the era of rapid information dissemination, this information can be spread to each individual in many ways. In the subsequent data reports, you can clearly see the number of infected people is declining, which means that media reports have a positive effect on the prevention of infectious diseases.

In this paper, although we have found that media impact could effectively control the spread of diseases in a certain range, we do not know how this media impact specifically affects the infectious disease system, and whether this media factor is the best for disease control. Therefore, we will spend a lot of time to study the specific links between media and infectious diseases in the future.

The obtained results could be beneficial for accurately assessing the effect of the media coverage in the control and treatment of infective diseases.

Acknowledgments

The authors are grateful to the anonymous reviewers for their constructive comments. This work is supported by the National Natural Science Foundation of China (Grant Nos. 11661050 and 11861044), and the HongLiu First-class Disciplines Development Program of Lanzhou University of Technology.

Conflict of interest

All authors declare no conflicts of interest in this paper.

References

1. A. L. Lloyd, V. A. A. Jansen, Spatiotemporal dynamics of epidemics: Synchrony in metapopulation models, *Math. Biosci.*, **188** (2004), 1–16.
2. M. Su, C. Hui, The effect of predation on the prevalence and aggregation of pathogens in prey, *Biosystems*, **105** (2011), 300–306.
3. C. Bret, Modeling and inference for infectious disease dynamics: A likelihood-based approach, *Stat. Sci.*, **33** (2018), 57–69.
4. G. Q. Sun, J. H. Xie, S. H. Huang, Z. Jin, M.-T. Li, L. Liu, Transmission dynamics of cholera: Mathematical modeling and control strategies, *Commun. Nonlin. Sci. Numer. Si.*, **45** (2017), 235–244.
5. Y. Kazuo, Threshold dynamics of reaction–diffusion partial differential equations model of Ebola virus disease, *Int. J. Biomath.*, **11** (2018), 1850108.
6. J. R. Petrella, W. R. Hao, A. Rao, P. M. Doraiswamy, Computational causal modeling of the dynamic biomarker cascade in alzheimer's disease, *Comput. Math. Methods Med.*, **2019** (2019), 6216530.
7. Q. Yang, H. F. Huo, Dynamics of an edge-based SEIR model for sexually transmitted diseases, *Math. Biosci. Eng.*, **17** (2020), 669–699.
8. D. M. Xiao, S. G. Ruan, Global analysis of an epidemic model with nonmonotone incidence rate, *Math. Biosci.*, **208** (2007), 419–429.
9. M. Haque, J. Zhen, E. Venturino, An ecoepidemiological predator-prey model with standard disease incidence, *Math. Method Appl. Sci.*, **32** (2010), 875–898.
10. L. I. Bo, S. L. Yuan, W. G. Zhang, Analysis on an epidemic model with a ratio-dependent nonlinear incidence rate, *Int. J. Biomath.*, **4** (2011), 227–239.
11. Y. L. Cai, W. M. Wang, Spatiotemporal dynamics of a reaction-diffusion epidemic model with nonlinear incidence rate, *J. Stat. Mech. Theory. E*, **2011**(2011), P02025.
12. X. B. Zhang, S. Q. Chang, H. Huo, Dynamic behavior of a stochastic SIR epidemic model with vertical transmission, *Electron. J. Differ. Equat.*, **2019**(2019), 1–20.
13. D. Wodarz, D. N. Levy, N. L. Komarova, Multiple infection of cells changes the dynamics of basic viral evolutionary processes, *Evolution*, **3** (2019), 104–115.
14. D. X. Jia, T. H. Zhang, S. L. Yuan, Pattern dynamics of a diffusive toxin producing phytoplankton-zooplankton model with three-dimensional patch,*Int. J. Bifurcat. Chaos*, **29** (2019), 1930011.
15. M. Bendahmane, M. Langlais, A reaction-diffusion system with cross-diffusion modeling the spread of an epidemic disease, *J. Evol. Equ.*, **10** (2010), 883–904.
16. W. Z. Huang, M. A. Han, K. Y. Liu, Dynamics of an SIS reaction-diffusion epidemic model for disease transmission, *Math. Biosci. Eng.*, **7** (2017), 51–66.
17. S. N. Zhao, S. L. Yuan, H. Wang, Threshold behavior in a stochastic algal growth model with stoichiometric constraints and seasonal variation, *J. Differ. Equat.*, **268** (2020), 5113–5139.
18. A. D'Onofrio, Stability properties of pulse vaccination strategy in SEIR epidemic model, *Math. Biosci.*, **179**(2002), 57–72.

19. M. DelaSen, S. Alonso-Quesada, R. Nistal, A. Ibeas, On the existence of equilibrium points, boundedness, oscillating behavior and positivity of a sveirs epidemic model under constant and impulsive vaccination, *Advances Differ. Equat.*, **2011** (2011), 339–370.
20. A. L. Shane, R. K. Mody, J. A. Crump, L. K. Pickering, 2017 infectious diseases society of America clinical practice guidelines for the diagnosis and management of infectious diarrhea, *Clin. Infect. Dis.*, **65**(2017), 1963–1973.
21. C. Kuttler, Modeling to inform infectious disease control, *Biometrics*, **74** (2018), 382–383.
22. S. K. Nandi, S. Jana, M. Mandal, K. K. Tapan, Complex dynamics and optimal treatment of an epidemic model with two infectious diseases, *Biosystems*, **5** (2019), 5–29.
23. C. Y. Zheng, C. Y. Xia, Q. T. Guo, M. Dehmer, Interplay between SIR-based disease spreading and awareness diffusion on multiplex networks, *J. Parallel Distr. Com.*, **115** (2018), 20–28.
24. L. J. S. Allen, B. M. Bolker, Y. Lou, A. L. Nevai, Asymptotic profiles of the steady states for an SIS epidemic patch model, *SIAM. J. Appl. Math.*, **67** (2007), 1283–1309.
25. R. H. Cui, Y. Lou, A spatial SIS model in advective heterogeneous environments, *J. Differ. Equat.*, **261** (2016), 3305–3343.
26. G. Q. Sun, J. Zhang, L. P. Song, Z. Jin, B. L. Li, Pattern formation of a spatial predator-prey system, *Appl. Math. Comput.*, **218** (2012), 11151–11162.
27. G. Q. Sun, L. Li, Z. K. Zhang, Spatial dynamics of a vegetation model in an arid flat environment, *Nonlin. Dynam.*, **73** (2013), 2207–2219.
28. D. Kalajdzievska, M. Y. Li, Modeling the effects of carriers on transmission dynamics of infectious diseases, *Math. Biosci. Eng.*, **8** (2017), 711–722.
29. F. Berezovskaya, G. Karev, B. J. Song, C. Castillo-Chvez, A simple epidemic model with surprising dynamics, *Math. Biosci. Eng.*, **2** (2005), 133–152.
30. X. W. Yu, S. L. Yuan, Asymptotic properties of a stochastic chemostat model with two distributed delays and nonlinear perturbation, *Discrete Cont. Dyn. Syst. B*, **25** (2020), 2373–2390.
31. X. Y. Meng, H. F. Huo, X. B. Zhang, Stability and global Hopf bifurcation in a Leslie-Gower predator-prey model with stage structure for prey, *J. Appl. Math. Comput.*, **60** (2019), 1–25.
32. X. Y. Meng, J. Li, Stability and Hopf bifurcation analysis of a delayed phytoplankton-zooplankton model with Allee effect and linear harvesting, *Math. Biosci. Eng.*, **17** (2020), 1973–2002.
33. X. Y. Meng, Y. Q. Wu, Dynamical analysis of a fuzzy phytoplankton-zooplankton model with refuge, fishery protection and harvesting, *J. Appl. Math. Comput.*, **63** (2020), 361–389.
34. W. M. Wang, Y. L. Cai, M. J. Wu, K. F. Wang, Z. Q. Li, Complex dynamics of a reaction-diffusion epidemic model, *Nonlin. Anal. Real Word Appl.*, **13** (2012), 2240–2258.
35. T. Wang, Dynamics of an epidemic model with spatial diffusion, *Phys. A*, **409** (2014), 119–129.
36. W. M. Wang, H. Y. Liu, Y. L. Cai, Z. Q. Li, Turing pattern selection in a reaction-diffusion epidemic model, *Chinese Phys. B*, **20** (2011), 074702.
37. M. Fras, M. Gosak, Spatiotemporal patterns provoked by environmental variability in a predator-prey model, *Biosystems*, **114** (2013), 172–177.

38. Z. P. Ma, H. F. Huo, H. Xiang, Spatiotemporal patterns induced by delay and cross fractional diffusion in a predator-prey model describing intraguild predation, *Math. Methods Appl. Sci.*, **43** (2020), 5179–5196.

39. A. Onofrio, M. Banerjee, P. Manfredi, Spatial behavioural responses to the spread of an infectious disease can suppress Turing and Turing-Hopf patterning of the disease, *Phys. A*, **545** (2020), 123773.

40. Y. F. Li, J. A. Cui, The effect of constant and pulse vaccination on SIS epidemic models incorporating media coverage, *Commun. Nonlin. Sci. Numer. Simul.*, **14** (2008), 2353–2365.

41. M. J. Ma, S. Y. Liu, J. Li, Does media coverage influence the spread of drug addiction, *Commun. Nonlinear Sci. Numer. Simul.*, **50**(2017), 169–179.

42. M. A. Khan, S. Islam, G. Zaman, Media coverage campaign in hepatitis b transmission model, *Appl. Math. Comput.*, **331** (2018), 378–393.

43. R. S. Liu, J. H. Wu, H. P. Zhu, Media/psychological impact on multiple outbreaks of emerging infectious diseases, *Comput. Math. Methods Med.*, **8** (2007), 153–164.

44. J. A. Cui, X. Tao, H. P. Zhu, An SIS infection model incorporating media coverage, *Rocky Mountauin J. Math.*, **38** (2008), 1323–1334.

45. Y. P. Liu, J. A. Cui, The impact of media coverage on the dynamics of infections disease, *Int. J. Biomath*, **1** (2008), 65–74.

46. Y. F. Li, J. A. Cui, The effect of constant and pulse vaccination on SIS epidemic models incorporating media coverage, *Commun. Nonlin. Sci. Numer. Simul.*, **14** (2009), 2353–2365.

47. J. A. Cui, Y. H. Sun, H. P. Zhu, The impact of media on the control of infectious diseases, *J. Dyn. Differ. Equ.*, **20** (2008), 31–53.

48. Y. N. Xiao, S. Y. Tang, J. H. Wu, Media impact switching surface during an infectious disease outbreak, *Sci. Rep.*, **5** (2015), 7838.

49. Q. L. Yan, S. Y. Tang, S. Gabriele, J. H. Wu, Media coverage and hospital notifications: Correlation analysis and optimal media impact duration to manage a pandemic, *J. Theor. Biol.*, **390** (2016), 1–13.

50. J. M. Tchuenche, N. Dube, B. P. Claver, J. S. Robert, T. B. Chris, The impact of media coverage on the transmission dynamics of human influenza, *BMC Public Health*, **11**(2011), S5.

51. C. J. Sun, W. Yang, J. Arino, K. Kamran, Effect of media-induced social distancing on disease transmission in a two patch setting, *Math. Biosci.*, **230** (2011), 87–95.

52. P. V. D. Driessche, J. Watmough, Reproduction numbers and sub-threshold endemic equilibria for compartmental models of disease transmission, *Math. Biosci.*, **180** (2002), 29–48.

53. X. Y. Meng, J. G. Wang, Analysis of a delayed diffusive model with Beddington-Deangelis functional response, *Int. J. Biomath.*, **12** (2019), 1950047.

54. Y. Zhao, J. Li, X. Ma, Stochastic periodic solution of a susceptible-infective epidemic model in a polluted environment under environmental fluctuation, *Comput. Math. Methods Med.*, **2018** (2018), 1–15.

AIMS Press